Production of massive lepton pairs in hadronic collisions*

H. B. Thacker
Institute for Theoretical Physics, State University of New York at Stony Brook, Stony Brook, New York 11790
(Received 19 November 1973)

The production of lepton pairs of large invariant mass in high-energy hadronic collisions is studied. A general method for treating the typical phase-space integrations that arise is derived and employed in subsequent model calculations. The general properties of annihilation models are discussed in an invariant context, and the various distributions are studied in a pion-annihilation model. The SU(3) properties of the quark-annihilation model are investigated and the cross section is related to deep-inelastic neutrino structure functions. A model is studied in which the lepton pair is emitted by a bremsstrahlung process, and a cancellation among the several graphs is seen to reduce the incident energy dependence by one power of s.

I. INTRODUCTION

The production of high-mass lepton pairs in hadronic collisions

$$p+p \to l^+ + l^- + \text{anything} \tag{1.1}$$

has recently become an object of both experimental and theoretical interest. Some data are available at BNL energies[1] and the experiment is being done at much higher energy at the CERN ISR. Though it may be some time before definitive measurements are available on the differential cross section of (1.1) and its dependence on initial energy and the four-momentum of the lepton pair, the potential importance of this process can hardly be overemphasized. It provides a point of direct contact between theoretical concepts which have arisen largely from the study of hadronic inclusive reactions and those concepts which were primarily motivated by the electromagnetic interactions of hadrons. To lowest order in the electromagnetic coupling constant, (1.1) represents the inclusive production of a virtual photon, and it has the same kinematical structure as a one-particle inclusive reaction. It will be interesting to find out whether the cross section exhibits the same features that characterize purely hadronic inclusive cross sections, e.g., sharp energy-independent falloff in transverse momentum and Feynman-Yang scaling in longitudinal momentum, and if so, how these distributions are affected by the photon mass variable. On the other hand, from the standpoint of electromagnetic theory, the cross section for (1.1) is determined by the matrix element of a current product between two-proton states and will provide important new tests of various ideas which have been formed about these products. For example, as has been emphasized by Jaffe,[2] this cross section can provide an indication as to what extent the parton description of electromagnetic currents can be taken literally and to what extent it is merely a convenient way of intuiting the light-cone singularity of a current product.

In this paper, the process (1.1) is studied from a variety of viewpoints. In view of our substantial ignorance of the detailed dynamics involved, the first part of this paper is devoted to some model-independent manipulations which will greatly facilitate the subsequent model calculations and which may perhaps be of some relevance even if all the models studied here prove false. The organization of the paper is as follows: In Sec. II the kinematics of (1.1) are briefly reviewed. Section III gives a general technique for performing integrations over the phase space of the final hadrons which frequently arise in model calculations. In Sec. IV a model is studied in which the lepton pair is produced by the peripheral annihilation of a π^+ from one proton with a π^- from the other proton. In Sec. V the Drell-Yan[3] model is discussed. Here the annihilating particles are assumed to be Gell-Mann–Zweig quarks, and particular attention is paid to the SU(3) structure and the connection it provides between (1.1) and deep-inelastic scattering results. Section VI discusses an alternative to the annihilation mechanism for the production of lepton pairs. In this model, which has previously been studied by Berman, Levy, and Neff,[4] the heavy virtual photon is produced by bremsstrahlung from one of the colliding hadrons. The results of Sec. VI suggest that such a mechanism may be relevant at large transverse momentum of the lepton pair.

II. KINEMATICS

Though the kinematics of (1.1) have been discussed elsewhere in the literature, we will review them here. This will also serve to introduce much of the notation and conventions to be

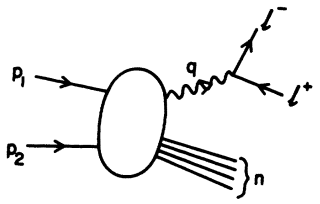

FIG. 1. Lepton-pair production to lowest order in α.

used in the remainder of the paper. All our considerations will be to lowest order in the electromagnetic coupling constant. To this order the reaction (1.1) occurs as in Fig. 1 and we can write the differential cross section summed over final hadronic states as

$$d\sigma = \frac{\alpha^2}{8\pi^4[s(s-4M^2)]^{1/2}q^4} W_{\mu\nu} L^{\mu\nu} d^4q , \tag{2.1}$$

where M is the nucleon mass, and the leptonic and hadronic tensors are given respectively by

$$L_{\mu\nu} = \int \frac{d^3k_1}{2k_{10}} \frac{d^3k_2}{2k_{20}} \delta^4(k_1+k_2-q)\,\mathrm{Tr}\not{k}_1\gamma_\mu\not{k}_2\gamma_\nu \tag{2.2}$$

and

$$\begin{aligned} W_{\mu\nu} &= \sum_n (2\pi)^4 \delta^4(p_1+p_2-p_n-q) \\ &\quad \times \langle p_1 p_2|J_\mu(0)|n\rangle\langle n|J_\nu(0)|p_1p_2\rangle \\ &= \int dx\, e^{-iqx}\, {}_{\text{in}}\langle p_1p_2|J_\mu(x)J_\nu(0)|p_1p_2\rangle_{\text{in}} \end{aligned} \tag{2.3}$$

(spin-averaging of the protons will always be implied). In (2.2) and throughout, the lepton mass is neglected. The subsequent discussion will also be greatly simplified by neglecting the nucleon mass, although for comparison with BNL data the effect of finite nucleon mass will be taken into account by an approximate procedure described in Sec. IV.

Since the leptonic tensor (2.2) is conserved and depends only on q, we may write

$$L_{\mu\nu} = (q_\mu q_\nu - q_{\mu\nu}q^2)\, L , \tag{2.4}$$

and since the hadronic tensor is also conserved, only the second term of (2.4) will contribute. By summing over Lorentz indices and doing the integrations in (2.2) we get $L = 2\pi/3$. Thus, the inclusive differential cross-section as a function of the four-momentum q of the lepton pair is related to the trace of the hadronic tensor by

$$\frac{d\sigma}{d^4q} = \frac{\alpha^2}{12\pi^3[s(s-4M^2)]^{1/2}q^2}(-W^\mu{}_\mu). \tag{2.5}$$

It is helpful to keep in mind the phase-space and spectral restrictions which limit the values of q accessible to (1.1). This is most easily discussed in terms of scalar invariants. Because of azimuthal symmetry, $W \equiv W^\mu{}_\mu$ is a function of three scalar invariants in addition to $s = (p_1+p_2)^2$. In most cases we will take the three independent variables to be q^2, $\nu_1 = p_1\cdot q$, and $\nu_2 = p_2\cdot q$, or their dimensionless counterparts

$$\omega = \frac{q^2}{s}, \quad \omega_1 = \frac{2\nu_2}{s}, \quad \omega_2 = \frac{2\nu_1}{s} . \tag{2.6}$$

The inverted choice of subscripts for ω_1 and ω_2 has its origins in the parton model, but for uniformity it will be adopted throughout. It will also be convenient to define the dimensionless transverse-momentum variable

$$\omega_\perp = \frac{q_\perp{}^2}{s} = \omega_1\omega_2 - \omega . \tag{2.7}$$

The positivity of the mass and energy of the hadronic final state requires

$$\omega_1 < 1, \quad \omega_2 < 1 , \tag{2.8}$$

$$1-\omega_1-\omega_2+\omega > 0 . \tag{2.9}$$

Similar restrictions on the lepton pair restrict the accessible values of these variables to

$$\omega, \omega_1, \omega_2 > 0 . \tag{2.10}$$

Finally, the physical region is confined to $\omega_\perp > 0$ or

$$\omega_1\omega_2 > \omega . \tag{2.11}$$

The combined restrictions (2.8)–(2.11) define a closed region in the three-dimensional space $(\omega, \omega_1, \omega_2)$.

III. PHASE-SPACE INTEGRALS

Before considering the details of particular models, some machinery will be developed for handling the typical phase-space integrals which arise in calculations of the inclusive cross section for (1.1). The procedure to be followed is inspired by annihilation-type models (parton or multiperipheral models), but it is developed in a model-independent way, and in Sec. VI the same formalism will be used to analyze the bremsstrahlung model.

The basic object of interest is the trace of expression (2.3) which we rewrite as

$$\begin{aligned} W &= W^\mu{}_\mu \\ &= \sum_n (2\pi)^4 \delta^4(p_1+p_2-p_n-q)\, B_n(p_1,p_2;p_i') , \end{aligned} \tag{3.1}$$

where

$$\begin{aligned} B_n(p_1,p_2;p_i') = \sum_\alpha &\langle p_1p_2|J_\mu(0)|n,\alpha\rangle \\ &\times\langle n,\alpha|J^\mu(0)|p_1p_2\rangle . \end{aligned} \tag{3.2}$$

The momenta of the particles in the n-particle state $|n, \alpha\rangle$ are designated by p_i', $i=1, 2, \ldots, n$. The summation in (3.1) of course includes an integration over n-particle phase space as well as a sum over particle number n. In (3.2) the sum is over the discrete quantum numbers α.

Now let us suppose that there is some natural decomposition of the squared matrix element B_n into a number of terms,

$$B_n = \sum_l B_{nl} . \tag{3.3}$$

For the time being this decomposition will be left unspecified. Let us refer to the set of particles in a state $|n, \alpha\rangle$ as $\{n\}$. Suppose now that we have selected the decomposition (3.3) of B_n in such a way that for each term B_{nl}, the particles $\{n\}$ fall naturally into two subsets $\{l\}$ and $\{l'\}=\{n\}-\{l\}$. A good illustrative example of what is meant here would be a simple multiperipheral model in which the production amplitude for photon $+n$ particles is given by the sum of graphs with all the various orderings of particles and photon along the multiperipheral chain. In the squared amplitude, interference terms between different orderings are neglected. In such a model, the terms in (3.3) would represent squared multiperipheral graphs, and for each of these terms, the subsets $\{l\}$ and $\{l'\}$ would consist of the particles on either side of the photon line, as in Fig. 2.

By introducing δ functions into (3.1) we will give a name to the total 4-momentum transfer between the initial proton p_1 and the final-state subset $\{l\}$ and also to the momentum transfer between p_2 and $\{l'\}$ (they will be called k and k', respectively). Thus (3.1) is rewritten as

$$W = \frac{1}{(2\pi)^4} \int d^4k\, G(k, -q-k, p_1, p_2) , \tag{3.4}$$

where

$$G(k, k', p_1, p_2) = \sum_n \sum_l (2\pi)^4 \delta^4 \left(p_1 + k - \sum_{i \in \{l\}} p_i' \right) \times (2\pi)^4 \delta^4 \left(p_2 + k' - \sum_{i \in \{l'\}} p_i' \right) \times B_{nl}(p_1, p_2; p_i') . \tag{3.5}$$

The form of the function G will depend on how we choose to divide up the particles for each piece of the squared amplitude, i.e., which partition of $\{n\}$ into $\{l\}$ and $\{l'\}$ is associated with each term B_{nl}. The whole point of these manipulations is that, by appropriate choice of these partitions, the expression on the right-hand side of (3.5) can often be calculated almost by inspection. (In the peripheral pion model of Sec. IV for example, G will be essentially the product of the absorptive parts of two π-p forward amplitudes.) Thus, the phase-space integral (3.4), with G being some known function, is the typical one that will be encountered when calculating W in particular models.

If p_1, p_2, and q are held fixed, $G(k, -q-k, p_1, p_2)$ can be written as a function of four invariants involving k. A convenient choice will be

$$t_1 = k^2 , \tag{3.6a}$$

$$t_2 = (q+k)^2 , \tag{3.6b}$$

$$\kappa_1 = 2p_1 \cdot k , \tag{3.6c}$$

$$\kappa_2 = -2p_2 \cdot (q+k) . \tag{3.6d}$$

Now we make the change of variables

$$d^4k = J^{-1}\, dt_1\, dt_2\, d\kappa_1\, d\kappa_2 , \tag{3.7}$$

where

$$J = \frac{\partial(t_1, t_2, \kappa_1, \kappa_2)}{\partial(k_0, k_1, k_2, k_3)} . \tag{3.8}$$

In the Appendix it is shown that J^{-1} can be written as

$$J^{-1} = \frac{\theta(-H)}{(-H)^{1/2}} , \tag{3.9}$$

where H is a determinant given in the Appendix. The equation $H=0$ defines a four-dimensional parabolic ellipsoid. (In the t_1-t_2 plane for fixed κ_1 and κ_2 the inequality $H<0$ corresponds to the interior of an ellipse.) The region $H<0$ is the physical region (i.e., to have $H>0$ would require complex values for the four-vector k), and the square-root singularity of the Jacobian (3.9) around the edge of the physical region is a well-known property of invariant phase space. In addition to the restriction to the physical region, we want to impose the condition that the invariant masses of the two subsets of final hadrons, i.e., $(p_1+k)^2$ and $(p_2-q-k)^2$, be positive. In terms of the integration variables (3.6), this means that

$$\kappa_1 + t_1 > 0, \quad \kappa_2 + t_2 > 0 . \tag{3.10}$$

These conditions truncate the physical region and

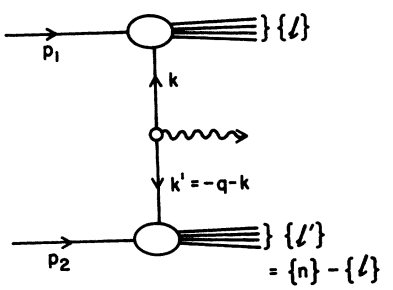

FIG. 2. Partition of final hadrons in multiperipheral model.

thus the integration in (3.4) is over a finite region.

It will be convenient to change κ_1, κ_2 to the dimensionless variables β_1, β_2, where

$$\beta_i = -\frac{t_i}{\kappa_i} . \tag{3.11}$$

Consider G in Eq. (3.4) to be a function of t_i and β_i. Thus

$$G(k, -q-k, p_1, p_2) \equiv G(t_1, t_2, \beta_1, \beta_2) . \tag{3.12}$$

G is also a function of the fixed invariants, e.g., s, ω, ω_1, and ω_2, but this dependence will be suppressed for now.

We are now faced with the integral

$$W = \frac{1}{(2\pi)^4} \int \frac{d\beta_1}{\beta_1^2} \frac{d\beta_2}{\beta_2^2} \theta(1-\beta_1)\,\theta(1-\beta_2) \times \int \frac{\theta(-H)}{(-H)^{1/2}} G(t_1, t_2, \beta_1, \beta_2) \times t_1\, dt_1\, t_2\, dt_2 . \tag{3.13}$$

The fact that the t_1-t_2 integration is over the interior of an ellipse makes expression (3.13) rather unenlightening even if the form of G is known. In order to work it into a more tenable representation, the inverse Laplace-transform function is introduced:

$$\mathcal{G}(b_1, b_2, \beta_1, \beta_2) = \frac{1}{(2\pi i)^2} \int_{-i\infty}^{i\infty} t_1\, dt_1\, t_2\, dt_2\, e^{-b_1 t_1 - b_2 t_2} \times G(t_1, t_2, \beta_1, \beta_2) . \tag{3.14}$$

Here it is assumed that G is given in a form which allows analytic continuation into the complex t_1 and t_2 planes. This is true of all the models to be studied here. More generally it would seem to be a reasonable assumption because, roughly speaking, the expression (3.5) for G represents an absorptive part in the s channel and thus should have an analytic form in the t-channel variables. (One would not expect G to contain, for example, θ or δ functions in t_1 or t_2.) Another thing which is true of all the models to be studied is that G has no singularities in the left half t_1 and t_2 planes. Thus we can assume that $G(b_1, b_2, \beta_1, \beta_2) = 0$ for $b_1 < 0$ or $b_2 < 0$. (Depending on the behavior of G as $t_1, t_2 \to -\infty$, G may contain δ functions or derivatives thereof at $b_1, b_2 = 0$.)

Writing G in terms of the inverse of (3.14) gives

$$W = \frac{1}{(2\pi)^4} \int_{-\infty}^{1} \frac{d\beta_1}{\beta_1^2} \frac{d\beta_2}{\beta_2^2} \int_0^\infty db_1\, db_2\, \mathcal{G}(b_1, b_2, \beta_1, \beta_2) I , \tag{3.15}$$

where

$$I = \int dt_1\, dt_2 \frac{\theta(-H)}{(-H)^{1/2}} e^{b_1 t_1 + b_2 t_2} . \tag{3.16}$$

The calculation of I requires some rather tedious manipulations which are described in the Appendix. The basic idea is to make a change of variables which converts the elliptical integration region $H < 0$ into a circle. Surprisingly, the resulting radial and angular integrations can be carried out analytically with no approximations. The result is

$$I = \frac{\pi \beta_1 \beta_2\, \theta[(\beta_1 - \omega_1)(\beta_2 - \omega_2) - \omega_\perp]}{4s(\kappa^2 - \beta_1 \beta_2 b_1 b_2 \omega_\perp)^{1/2}} \times e^{-s\kappa} \sinh[s(\kappa^2 - \beta_1 \beta_2 b_1 b_2 \omega_\perp)^2] , \tag{3.17}$$

where κ is given below in (3.19).

To recapitulate, we have now derived the following model-independent representation for W:

$$W = \frac{1}{16\pi^3 s} \int_0^1 \frac{d\beta_1}{\beta_1} \frac{d\beta_2}{\beta_2} \int_0^\infty db_1\, db_2\, \mathcal{G}(b_1, b_2, \beta_1, \beta_2) \frac{\theta[(\beta_1 - \omega_1)(\beta_2 - \omega_2) - \omega_\perp]}{4(\kappa^2 - \beta_1 \beta_2 b_1 b_2 \omega_\perp)^{1/2}} e^{-s\kappa} \sinh[s(\kappa^2 - \beta_1 \beta_2 b_1 b_2 \omega_\perp)^{1/2}] , \tag{3.18}$$

where

$$\kappa = \tfrac{1}{2}[\beta_1(\beta_2 - \omega_2) b_1 + \beta_2(\beta_1 - \omega_1) b_2] . \tag{3.19}$$

This expression, though formidable in appearance, will prove to be very helpful in studying the behavior of the differential cross section in models, particularly when considering various asymptotic limits. The complicated boundaries of phase space have been obviated, and only simple parametric integrals remain. The dependence on the four-momentum q now appears in terms of the invariants ω_1, ω_2, and $\omega_\perp$, making the study of invariant distributions a straightforward matter once the function $\mathcal{G}$ is determined.

A limiting form of (3.18) which is of particular interest is that obtained by holding $q_\perp^2$ fixed and letting s become large, i.e., its behavior for $\omega_\perp \ll 1$. This covers a considerable amount of the experimentally interesting region. (For example, even at $q_\perp^2$ as large as 10 GeV^2 we would have $\omega_\perp \approx 0.2$ at BNL and $\omega_\perp \approx 0.005$ at ISR.) Barring unusual behavior of $\mathcal{G}$ at $b_1, b_2 \approx 0$ [in which case we must revert back to the exact expression (3.18)], W can be written in this limit as

$$W=\frac{1}{16\pi^3 s}\int_{\omega_1}^{1}\frac{d\beta_1}{\beta_1}\int_{\omega_2}^{1}\frac{d\beta_2}{\beta_2}\int_0^\infty\frac{db_1\,db_2}{8\kappa}\,\mathcal{G}(b_1,b_2,\beta_1,\beta_2)\,e^{-(\beta_1\beta_2 b_1 b_2/2\kappa)q_\perp^2},\qquad q_\perp^2\ll s\,. \tag{3.20}$$

Finally, it should be emphasized that the usefulness of the representation (3.18) or (3.20) depends on the ease with which the function G can be calculated. Although in principle one can always cast W in the form (3.18), from a practical standpoint, the evaluation of G will typically involve the assumption that interference terms arising from the phase-space overlap of the two final-state subsets can be neglected.

IV. PERIPHERAL-PION ANNIHILATION MODEL

In this section a model will be considered in which the lepton pairs are produced via the annihilation of two virtual charged pions as pictured in Fig. 3.[5,6] This model has some similarity to the Drell-Yan quark-parton model (which will be discussed in Sec. V). Among the major differences are the following: (1) The annihilating particles have spin-0 instead of the usual spin-$\frac{1}{2}$ partons, (2) we expect some electromagnetic structure at the $\pi\pi\gamma$ vertex as opposed to the usual pointlike assumption of the parton model, and (3) we are dealing with the exchange of a well-known particle instead of a hypothetical one. In connection with the last point it can be said that, without any predisposition as to the appropriateness of Fig. 3 as a model for lepton-pair production, it is at least of interest to determine how large a contribution can be expected from virtual-pion annihilation. There is no *a priori* reason to expect Fig. 3 to be suppressed at large s and q^2 (except by the q^2 dependence of the pion form factor), since even in this region it is still kinematically possible for both pions to be near the mass shell.

A. The model

Each n-particle + lepton pair production process is assumed to take place as in Fig. 3. Each B_n can then be written as a sum of terms like that shown in Fig. 2. Thus

$$B_n=\sum_l\langle l|\phi_{\pi^+}(0)|p_1\rangle|^2\,|\langle n-l|\phi_{\pi^-}(0)|p_2\rangle|^2 \times\Gamma^\mu(-k,-k')\,\Gamma_\mu^*(-k,-k') +(p_1\rightleftharpoons p_2), \tag{4.1}$$

where $k=P_i-p_1$, $k'=P_i'-p_2$, and Γ_μ is the pion electromagnetic vertex function. To calculate G for this model, we insert (4.1) into (3.5) and observe that the states $|l\rangle\langle l|$ and $|n-l\rangle\langle n-l|$, when summed over both n and l, constitute two complete sets of intermediate states. Thus G becomes

$$G(k,k',p_1,p_2)=\frac{A_{\pi^+p}(p_1,k)}{(k^2-m_\pi^2)^2}\,\frac{A_{\pi^-p}(p_2,k')}{(k'^2-m_\pi^2)^2} \times\Gamma^\mu(-k,-k')\,\Gamma_\mu^*(-k,-k') +(p_1\rightleftharpoons p_2), \tag{4.2}$$

where the absorptive part of the π-p forward amplitude is defined as

$$A_{\pi^+p}(p,k)=\int dx\,e^{ikx}\langle p|j_{\pi^-}(x)j_{\pi^+}(0)|p\rangle\,. \tag{4.3}$$

When the pion is on the mass shell, (4.3) is related to the total π-p cross section (neglecting the pion mass):

$$A_{\pi^\pm p}(p,k)=4p\cdot k\,\sigma_{\pi^\pm p},\qquad k^2=m_\pi^2\,. \tag{4.4}$$

Since we are not primarily interested in detailed numerical evaluations, the π-p cross sections will be approximated by a constant

$$\sigma_{\pi^+p}\approx\sigma_{\pi^-p}\approx\text{const}\approx 24\text{ mb}. \tag{4.5}$$

Now let us assume that the pion can be taken off the mass shell by multiplying (4.4) by some cutoff function which depends only on the pion mass, i.e.,

$$A_{\pi p}(p,k)=4p\cdot k\,\sigma_{\pi p}F(k^2-m_\pi^2), \tag{4.6}$$

where (4.4) requires that $F(0)=1$. Since the cutoff function F will suppress contributions from highly virtual pions, the electromagnetic vertex functions in (4.2) can presumably be approximated, for large q^2, by their value for on-mass-shell pions:

$$\Gamma^\mu(-k,-k')\,\Gamma_\mu^*(-k,-k')=-q^2\,|F_\pi(q^2)|^2\,, \tag{4.7}$$

where $q=-k-k'$ and the pion mass has been neglected.

Inserting (4.6) and (4.7) into (4.2), setting $k'=-k-q$, and expressing G as a function of the variables t_1, t_2, β_1, β_2, and q^2, where the first four are defined in (3.6) and (3.11), we get

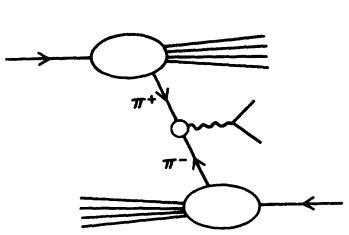

FIG. 3. Lepton-pair production via pion annihilation.

$$G(t_1, t_2, \beta_1, \beta_2) = -q^2 |F_\pi|^2 \sigma_{\pi p}{}^2 \frac{8 t_1 t_2}{\beta_1 \beta_2} \times \frac{F(t_1 - m_\pi{}^2)}{(t_1 - m_\pi{}^2)^2} \frac{F(t_2 - m_\pi{}^2)}{(t_2 - m_\pi{}^2)^2} . \tag{4.8}$$

In order to use the formulas of Sec. III, the inverse Laplace-transform function (3.14) must be found. Using (4.8) and ignoring $m_\pi{}^2$ when it is safe gives

$$\mathcal{G}(b_1, b_2, \beta_1, \beta_2) = \frac{-8q^2 |F_\pi|^2 \sigma_{\pi p}{}^2}{\beta_1 \beta_2} \mathcal{F}(b_1) \mathcal{F}(b_2) , \tag{4.9}$$

where F is the inverse transform of the cutoff function

$$\mathcal{F}(b) = \frac{1}{2\pi i} \int_{-i\infty}^{i\infty} dt\, F(t - m_\pi{}^2) e^{-bt} . \tag{4.10}$$

With (4.9) and (4.10) the invariant distributions in q^2, $q_\perp{}^2$, and longitudinal momentum or rapidity can now be studied.

B. Mass and longitudinal-momentum distribution

If the cutoff in the pion mass t_1 and t_2 is strong enough, the mass (q^2) and longitudinal-momentum distribution of the cross section (integrated over $q_\perp{}^2$) can be discussed without specifying the details of the cutoff function. First note that

$$\frac{d^2\sigma}{dq^2\, dy} = \frac{\pi}{2} \int \frac{d\sigma}{d^4 q} dq_\perp{}^2 = -\frac{\sigma^2}{24\pi^2 s q^2} \int W\, dq_\perp{}^2 , \tag{4.11}$$

where the differential cross section is considered as a function of q^2, $q_\perp{}^2$, and the longitudinal rapidity of the photon

$$y = \frac{1}{2} \ln \frac{\omega_1}{\omega_2} . \tag{4.12}$$

Now, if we were to use the exact expression (3.18) for W and do the $q_\perp{}^2$ integration first, the limits of integration would be

$$0 \leq q_\perp{}^2 \leq s(\beta_1 - \omega_1)(\beta_2 - \omega_2) . \tag{4.13}$$

However, it will be seen shortly that the cutoff in pion mass gives rise to a similar energy-independent cutoff in $q_\perp{}^2$. Therefore, if the cutoff is strong enough, as s gets large the upper limit on the $q_\perp{}^2$ integration can be ignored. Also, when s becomes large the only significant contribution to the $q_\perp{}^2$ integration comes from $q_\perp{}^2 \ll s$ (provided that the cutoff is strong enough to make this integral converge). Thus we may use, instead of (3.18), the $\omega_\perp \ll 1$ approximation (3.20). Observing that the function $\mathcal{G}$ in this model is independent of $q_\perp{}^2$, we get

$$\int W\, dq_\perp{}^2 = \frac{1}{2(2\pi)^3 s} \times \int_{\omega_1}^1 \frac{d\beta_1}{\beta_1{}^2} \int_{\omega_2}^1 \frac{d\beta_2}{\beta_2{}^2} \int_0^\infty \frac{db_1}{b_1} \frac{db_2}{b_2} \times \mathcal{G}(b_1, b_2, \beta_1, \beta_2) . \tag{4.14}$$

Now using the expression (4.9) for $\mathcal{G}$ and defining the quantity

$$\frac{1}{\Omega} = \int_0^\infty \frac{db}{b} \mathcal{F}(b) , \tag{4.15}$$

where $\mathcal{F}(b)$ is given in terms of the cutoff function F by (4.10), the partially integrated cross section is

$$\frac{d^2\sigma}{dq^2\, dy} = \frac{\alpha^2 \sigma_{\pi p}{}^2}{12(2\pi)^5 \Omega^2} \frac{|F_\pi(q^2)|^2}{2q^4} (1 - \omega_1{}^2)(1 - \omega_2{}^2) . \tag{4.16}$$

For notational simplicity we have left part of the right-hand side of (4.16) in terms of ω_1 and ω_2. However, these quantities are now functions of $q^2 = \omega s$ and y given by

$$\omega_1 = \sqrt{\omega}\, e^y \tag{4.17a}$$

$$\omega_2 = \sqrt{\omega}\, e^{-y} . \tag{4.17b}$$

We can now be more precise about what constitutes a "strong enough" cutoff in the pion mass. The procedure we used to carry out the $q_\perp{}^2$ integration as $s \to \infty$ is legitimate provided that the result, Eq. (4.14), does not diverge. Such divergence can only arise from the b_1 and b_2 integrals, or, more specifically, only if the integral (4.15) diverges. A divergence from the $b = \infty$ end of the integral would be an infrared-type divergence which would only occur if there were a massless ($k^2 = 0$) pole in the π-p forward amplitude, as can be seen by referring back to Eqs. (4.6) and (4.10). This possibility can safely be ignored. Thus, the only requirement needed to validate our procedure is that the integral (4.15) converge at the lower end, i.e., that

$$\mathcal{F}(b) \lesssim b^\epsilon \text{ as } b \to 0 \quad (\epsilon > 0) . \tag{4.18}$$

For a sufficiently nonpathological cutoff function, we may infer from (4.18) and the definition (4.10) that the asymptotic behavior of the cutoff function must satisfy

$$|F(t)| \lesssim |t|^{-1-\epsilon} , \tag{4.19}$$

as $t \to \infty$ in the left half plane, in order for the discussion in this section to be valid. As we will see

in Sec. IV C, a cuttoff satisfying (4.19) corresponds to a transverse-momentum falloff faster than $(q_\perp{}^2)^{-1-\epsilon}$. Actually, the discussion here is completely general since a cutoff at least as strong as (4.19) is necessary to ensure the gauge invariance of Fig. 3 to leading order in s.

By integrating (4.16) over rapidity we obtain the following result for the lepton-pair mass distribution

$$\frac{d\sigma}{dq^2} = \frac{\alpha^2 \sigma_{\pi p}{}^2}{6(2\pi)^5 \Omega^2} \frac{|F_\pi(q^2)|^2}{4q^4} f(\omega), \tag{4.20}$$

where the "scaling function" $f(\omega)$ is given by

$$f(\omega) = (1+\omega^2)\ln\frac{1}{\omega} - (1-\omega^2). \tag{4.21}$$

From (4.20) it is seen that $d\sigma/dq^2$ exhibits a Drell-Yan–type scaling behavior only if the electromagnetic structure of the pion is asymptotically pointlike, i.e., if

$$|F_\pi(q^2)|^2 \approx \text{const} \neq 0 \text{ as } q^2 \to \infty .$$

Between $(q^2)^{1/2} = 1$ to 2.5 GeV, the pion form factor is reasonably described by the formula[7]

$$|F_\pi(q^2)| \approx \frac{2}{q^2} \quad (q^2 \text{ in GeV}^2). \tag{4.22}$$

Using this along with (4.20), we obtain at $s = 55$ GeV^2 the q^2 and laboratory longitudinal-momentum distributions[8] shown in Figs. 4 and 5, with the parameter Ω fixed at

$$\Omega = 0.125 \text{ GeV}^{-2}. \tag{4.23}$$

Data from the Brookhaven experiment at the same energy are included for comparison. Also shown in Fig. 4 is the predicted q^2 distribution for a typical ISR energy of $s = 2500$ GeV^2. [It will be seen in Sec. IV C that the value of Ω in (4.23) corresponds to a rather slow falloff in transverse momentum, which is in agreement with experiment.[1]] In the distributions at $s = 55$ GeV^2, the effect of finite nucleon mass is far from negligible. (For example, the variable $\omega = q^2/s$ is limited to be $\lesssim 0.6$ instead of 1.) To account for this, the modified scaling variable

$$\omega' = 1 - \frac{1}{s}\Delta^{1/2}(s, q^2, 4M^2) \tag{4.24}$$

has been used in (4.21) instead of q^2/s.[9] Here, Δ is the well-known function

$$\Delta(a, b, c) = a^2 + b^2 + c^2 - 2ab - 2ac - 2bc . \tag{4.25}$$

The variable ω' has the right threshold properties (i.e., it always ranges from 0 to 1) and approaches ω in the limit of large s and q^2.

A few comments about the q^2 distribution are in order. Expression (4.20) has only been plotted for $(q^2)^{1/2} < 2.5$ GeV, where the pion form factor has been measured. It is clear that if the formula (4.22) is assumed to hold above 2.5 GeV, the prediction will be lower than the Brookhaven data by an order of magnitude or more in this region. Several possibilities come to mind: (1) It can easily be seen that, as q^2 gets larger, smaller invariant-mass values of the two π-p systems are emphasized.[10] In this region the πp cross section is, on the average, substantially larger than the approx-

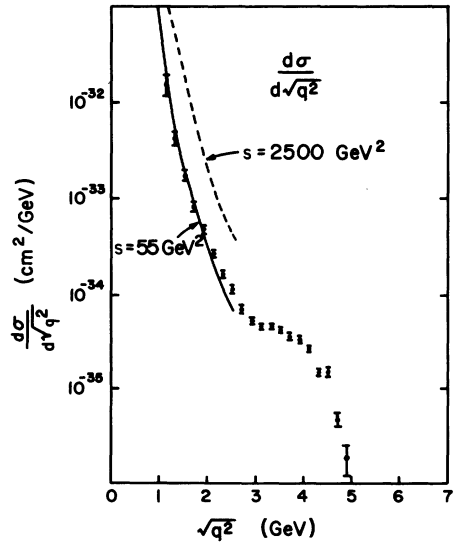

FIG. 4. Mass distribution predicted from peripheral-pion model. Data points are from Ref. 1.

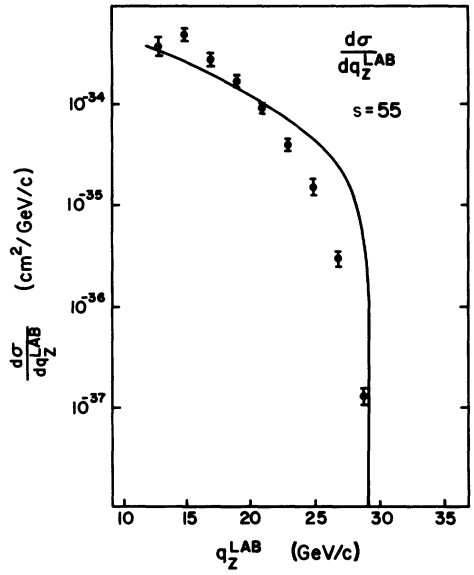

FIG. 5. Laboratory longitudinal-momentum distribution predicted from peripheral-pion model. Data points are from Ref. 1.

imation (4.5). This would result in an enhancement at larger values of q^2. However, rough calculations indicate that this effect is not large enough to account for the "shoulder" in the Brookhaven data. (2) It is possible that the pion form factor above $(q^2)^{1/2} = 2.5$ GeV is much larger than would be expected by extrapolating (4.22). (This possibility is mentioned with an utter lack of conviction.) (3) Finally, it may be that the pion-annihilation picture, if it has any validity, is only good at fairly low values of q^2, with entirely different physics taking over above a few GeV^2.

C. Transverse-momentum distribution

In Sec. IV B it was shown that, provided the pion mass cutoff $F(k^2 - m_\pi^2)$ was strong enough, the distribution in q^2 and in longitudinal momentum for large s was determined up to an over-all constant. [It might be noted that the crucial assumption that allowed us to gain this much information without specifying F was (4.6), which states that the pion mass dependence of the π-p forward amplitude factors out as an energy-independent cutoff.] Much less can be said about the transverse-momentum distribution because of the fact that it is so closely related to the specific form of the cutoff function. We will thus confine the discussion in this section to illustrating the relationship between the behavior of $F(k^2 - m_\pi^2)$ and the $q_\perp^2$ behavior of the cross section, without attempting to construct a model for either one.

The main points to be made in this section are well illustrated by considering an exponential cutoff function

$$F(t - m_\pi^2) = e^{\Omega(t - m_\pi^2)} . \tag{4.26}$$

Laplace-transforming this as in (4.10) and ignoring the pion mass, we get

$$\mathfrak{F}(b) = \delta(b - \Omega) . \tag{4.27}$$

Since the cutoff function is obviously strong enough to satisfy (4.18) or (4.19), the only experimentally interesting region as $s \to \infty$ is $\omega_\perp \ll 1$. Note also that in this region the restriction $\omega_1 \omega_2 \approx \omega$ applies, and so we need not worry about our choice of independent variables other than q^2. Now, using (4.27), (4.9), and (3.20) the transverse-momentum dependence of the cross section for fixed ω_1 and ω_2 is given by (leaving out $q_\perp^2$-independent factors)

$$W \sim \int_{\omega_1}^1 \frac{d\beta_1}{\beta_1^3} \int_{\omega_2}^1 \frac{d\beta_2}{\beta_2^3} \left[\left(1 - \frac{\omega_2}{\beta_2}\right) + \left(1 - \frac{\omega_1}{\beta_1}\right) \right]^{-1} \exp\left\{ -\left[\frac{\Omega}{(1 - \omega_1/\beta_1) + (1 - \omega_2/\beta_2)} q_\perp^2 \right] \right\} . \tag{4.28}$$

Without carrying out this integral, it can be seen that the cross section falls off exponentially in $q_\perp^2$, since the coefficient of $q_\perp^2$ in the exponent of (4.28) is never less than $\frac{1}{2}\Omega$. The leading $q_\perp^2$ behavior of (4.28) comes from $\beta_1 \approx 1$, $\beta_2 \approx 1$, where the coefficient in the exponent is smallest. Thus, the leading transverse-momentum behavior is roughly

$$W \sim \exp\left\{ -\left[\frac{\frac{1}{2}\Omega}{(1 - \sqrt{\omega}\cosh y)} q_\perp^2 \right] \right\} , \tag{4.29}$$

where we have again dropped $q_\perp^2$-independent factors, and have reintroduced the rapidity variable, using (4.17).

For fixed ω the transverse-momentum falloff is slowest in the central region $y \approx 0$, becoming increasingly sharp as we move toward larger values of rapidity. [This should be compared with the observed inclusive spectra of ordinary hadrons, in which the transverse-momentum falloff is more or less uncorrelated with the rapidity. Expression (4.29) is in accord with this observation, since, for ordinary hadrons, $\omega = m^2/s \approx 0$ and the cutoff (4.29) does indeed become essentially independent of rapidity.]

For fixed rapidity, the transverse-momentum falloff is slowest for small values of ω and becomes steeper as ω gets larger. This is in marked contrast to the model of Etim *et al.*[11] which supposes that the cross section scales in the variable $x_\perp \equiv q_\perp^2/q^2$ and thus has an average transverse momentum which increases with q^2.

So far we have considered only an exponential cutoff function. In order to discuss the $q_\perp^2$ behavior in somewhat more generality, we define the Mellin-transform function

$$M(\xi) = \int_0^\infty dq_\perp^2 (q_\perp^2)^{\xi - 1} W(q_\perp^2) , \tag{4.30}$$

suppressing, for the time being, the dependence of W on the other variables. We will assume throughout this section that, for large s, the $q_\perp^2$ falloff is rapid enough that we can safely use the $\omega_\perp \ll 1$ approximation (3.20). Noting that G is independent of $q_\perp^2$ for fixed ω_1 and ω_2 (and thus fixed ω), the Mellin transform can be written

$$M(\xi) = \frac{\Gamma(\xi)}{2(2\pi)^3 s} \int_{\omega_1}^1 \frac{d\beta_1}{\beta_1^2} \int_{\omega_2}^1 \frac{d\beta_2}{\beta_2^2} \int_0^\infty \frac{db_1}{b_1} \frac{db_2}{b_2} \mathcal{G}(b_1, b_2, \beta_1, \beta_2) \left[\left(1 - \frac{\omega_1}{\beta_1}\right) \frac{1}{b_1} + \left(1 - \frac{\omega_2}{\beta_2}\right) \frac{1}{b_2} \right]^{\xi - 1} . \tag{4.31}$$

The function W is recovered from its Mellin transform via the inverse of (4.30):

$$W(q_\perp^2)=\frac{1}{2\pi i}\int_{-i\infty}^{i\infty} d\zeta (q_\perp^2)^{-\zeta} M(\zeta). \tag{4.32}$$

The leading falloff in $q_\perp^2$ (i.e., the behavior as $q_\perp^2$ becomes greater than some fixed mass parameter in G, but still $\ll s$) is thus determined by the nearest singularity of $M(\zeta)$ in the right half ζ plane. Such a singularity must arise from the b_1 and b_2 integrations in (4.31). As discussed previously, divergences from the upper end of the b integrations correspond to infrared divergences, which we need not consider. Now, let us suppose that the cutoff function $F(t)$ falls off like a power of t for $|t|$ greater than some fixed mass parameter Ω^{-1}:

$$F(t)\sim \text{const}\times(\Omega t)^{-1-\alpha}, \quad \text{for } |t|>\Omega^{-1} \tag{4.33}$$

and we will assume that $\alpha>0$, so that the cutoff is "strong enough" as defined in (4.19). From the definition (4.10), the small-b behavior of $\mathfrak{F}(b)$ is determined to be

$$\mathfrak{F}(b)\sim \text{const}\times\Omega^{-1}\left(\frac{b}{\Omega}\right)^{\alpha}, \quad \text{for } b\lesssim\Omega. \tag{4.34}$$

Going back to (4.31), we can see that the nearest right-half-plane singularity of $M(\zeta)$ occurs at $\zeta=1+\alpha$. From (4.32), the leading transverse-momentum behavior is then

$$W\propto(q_\perp^2)^{-1-\alpha}. \tag{4.35}$$

Thus, a power-law cutoff in the pion mass gives rise to a transverse-momentum falloff of the same power.

The discussion after (4.29) of the q^2 and y dependence of the $q_\perp^2$ cutoff can be put on a more general basis by defining the average transverse momentum for fixed q^2 and y:

$$\langle q_\perp^2\rangle=\frac{\int_0^\infty dq_\perp^2\, q_\perp^2 W(q_\perp^2)}{\int_0^\infty dq_\perp^2 W(q_\perp^2)}$$

$$=\frac{M(2)}{M(1)}, \tag{4.36}$$

assuming that these integrals converge. Using expression (4.31) for the Mellin transform and using (4.9) for $\mathcal{G}$, the average transverse momentum as a function of mass and rapidity is determined up to an over-all constant:

$$\langle q_\perp^2\rangle=\text{const}\times\frac{1}{(1-\omega_1^2)(1-\omega_2^2)}$$

$$\times[3(1-\omega_1^2)(1-\omega_2^2)-(1-\omega_1^2)(1-\omega_2^3)$$

$$-(1-\omega_1^3)(1-\omega_2^2)], \tag{4.37}$$

where ω_1 and ω_2 are given in terms of ω and y by (4.17). This expression has the same qualitative behavior as that which would follow from (4.29), i.e., the average transverse momentum is largest when both ω and y are small and decreases as either ω or $|y|$ increases.

To summarize this section, although it is not possible to specify the $q_\perp^2$ distribution without choosing a specific cutoff function, we can make the following general statements: (1) The leading falloff of the cross section for large $q_\perp^2$ (but still $q_\perp^2\ll s$) is the same as the leading falloff of $F(t)$ for large t; and (2) the average transverse momentum as a function of mass and rapidity is given by (4.37). For fixed rapidity $\langle q_\perp^2\rangle$ decreases with increasing ω. For fixed ω, $\langle q_\perp^2\rangle$ decreases with increasing y. For fixed ω and y, $\langle q_\perp^2\rangle$ is independent of s.

V. THE QUARK-ANNIHILATION MODEL

The idea that the electromagnetic structure of the proton might be described as a collection of electromagnetically pointlike partons was given impetus by the famous scaling results of the SLAC-MIT electroproduction experiments. From this point of view, the scaling behavior of the structure functions at large energy and momentum transfer is an indication that there is no structure at the parton-photon vertex, and the scaling function $F_2(\omega)$ is a measure of the longitudinal-momentum distribution of the partons in a single proton state boosted to infinite momentum. The most well known and well studied, and probably the most reasonable, of these models is the quark-parton model, with spin-$\frac{1}{2}$ Gell-Mann–Zweig quarks. One of the most satisfying features of this model is that the electromagnetic and weak currents exhibit the desired SU(3) properties.

The quark-parton model has been extended to massive-lepton–pair production by several authors.[3,12] The central results of these investigations will be shown in this section to follow in a straightforward way from the formalism of Sec. III. In addition, we will give a more extensive analysis of the SU(3) properties of this model than has previously been available in the literature. Using a nonet-symmetry assumption (which amounts to the supposition that the proton contains no strange quarks), it will be possible to write the cross section for lepton-pair production entirely in terms of neutrino and antineutrino deep-inelastic structure functions with no adjustable parameters.

According to the assumptions of this model, the lepton-pair production process takes place via quark-antiquark annihilation, as shown in Fig. 6. In a manner very similar to the pion-annihilation

model of Sec. IV, the function G (defined in Sec. III) for this model will be essentially the product of two quark-proton forward amplitudes. But in order to obtain useful results, we want to relate the cross section to the structure functions for deep-inelastic scattering, which, in the parton model, are also determined by the quark-proton forward amplitudes. It is therefore necessary to briefly review the parton-model description of deep-inelastic scattering and derive some convenient formulas for the structure functions.

A. Review of deep-inelastic scattering

As is well known, the cross section for inclusive electroproduction or neutrino-induced production is determined by current products of the form

$$W^{ab}_{\mu\nu} = \int dx\, e^{iqx} \langle p | J^a_\mu(x) J^b_\nu(0) | p \rangle \ , \tag{5.1}$$

where J^a_μ and J^b_μ are either vector or axial-vector U(3) currents. To conform to standard notation, we use the symbol $W^{ab}_{\mu\nu}$ (in this subsection only) to represent the inelastic lepton scattering amplitude. It should not be confused with the $W_{\mu\nu}$ of the rest of the text, which refers to lepton-pair production. In the quark model, the U(3) currents appearing in (5.1) are given in terms of quark fields by

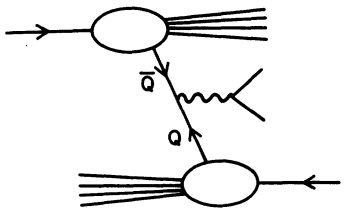

FIG. 6. Lepton-pair production via quark annihilation.

$$J^a_\mu = \bar\psi \Gamma_\mu (\tfrac{1}{2}\lambda_a)\psi = \bar\psi^i_\alpha \psi^j_\beta (\Gamma_\mu)_{\alpha\beta} (\tfrac{1}{2}\lambda_a)^{ij} \ , \tag{5.2}$$

where Γ_μ is either γ_μ or $\gamma_5\gamma_\mu$. The second expression in (5.2) is written simply to exemplify the conventions to be used in this section for the various indices which will appear. They are that (1) lower case Greek subscripts α, β, γ, ... are Dirac indices; (2) lower case letters a, b, c, ... are U(3) component indices running from 0 to 8; and (3) lower case letters i, j, k, ... are U(3) matrix indices running from 1 to 3.

The current product (5.1) thus involves four quark fields. According to standard parton-model arguments, the leading terms in the scaling limit are the semidisconnected pieces, where two of the quark fields contract to form a free propagator. Thus, neglecting masses,

$$W^{ab}_{\mu\nu} = \tfrac{1}{4} \int dx\, e^{iqx} [\langle p | \bar\psi^i_\alpha(x) \psi^l_\delta(0) | p \rangle (\Gamma_\mu \gamma_\sigma \Gamma_\nu)_{\alpha\delta} (\lambda_a \lambda_b)^{il} + \langle p | \psi^j_\beta(x) \bar\psi^k_\gamma(0) | p \rangle (\Gamma_\nu \gamma_\sigma \Gamma_\mu)_{\gamma\beta} (\lambda_b \lambda_a)_{kj}] \partial^\sigma \Delta_+(x) \ , \tag{5.3}$$

where the free-field function is defined to be

$$\Delta_+(x) = \frac{i}{(2\pi)^3} \int d^4k\, \theta(k_0)\, \delta(k^2)\, e^{-ikx} \ . \tag{5.4}$$

Defining the momentum-space quark-proton amplitudes

$$M^{ij}_{\alpha\beta}(p,k) = \int dx\, e^{ikx} \langle p | \bar\psi^j_\beta(x) \psi^i_\alpha(0) | p \rangle \tag{5.5}$$

and

$$\bar M^{ij}_{\alpha\beta}(p,k) = \int dx\, e^{ikx} \langle p | \psi^i_\alpha(x) \bar\psi^j_\beta(0) | p \rangle \ , \tag{5.6}$$

the amplitude (5.3) can be written

$$W^{ab}_{\mu\nu} = \frac{1}{4} \frac{1}{(2\pi)^3} \int d^4k\, \theta(q_0 - k_0)\, \delta((q-k)^2) \times [(\lambda_a \lambda_b)^{il} \operatorname{Tr}(M^{li} \Gamma_\mu (\not q - \not k) \Gamma_\nu) + (\lambda_b \lambda_a)^{kj} \operatorname{Tr}(\bar M^{jk} \Gamma_\nu (\not q - \not k) \Gamma_\mu)] \ . \tag{5.7}$$

In this expression and throughout, the symbol Tr will indicate the trace over Dirac indices, whereas tr will indicate the trace over SU(3) matrix indices. The M's inside the traces in (5.7) are of course Dirac matrices.

In order to simplify (5.7) it is convenient to introduce the contractions

$$\tfrac{1}{4} \operatorname{Tr}(M^{ij} \gamma_\mu) = M^{ij}_1 p_\mu + M^{ij}_2 k_\mu \tag{5.8}$$

and a similar expression with everything barred. The Dirac matrix M^{ij} may be written as

$$M^{ij}_{\alpha\beta} = M^{ij}_1 (\not p)_{\alpha\beta} + M^{ij}_2 (\not k)_{\alpha\beta} + \cdots \ . \tag{5.9}$$

The remaining terms in (5.9) involve scalar, tensor, axial-vector, and pseudoscalar Dirac matrices. The axial-vector and pseudoscalar terms can be eliminated on the basis of parity conservation. By substituting a scalar or tensor Dirac matrix into (5.7), it can be seen that these terms do not contribute to the scaling limit. Thus, the terms written in (5.9) are the only ones we need retain.

The quantities M_1^{ij} and M_2^{ij} depend on two scalar invariants formed from k. Let us take these to be

$$t = k^2 , \tag{5.10a}$$

$$\beta = -\frac{k}{2p\circ k} . \tag{5.10b}$$

A fundamental assumption of the parton model is that the quark amplitudes decrease precipitously in the quark mass variable k^2. Changing integration variables in (5.7) then allows us to write [see discussion after (5.12)]

$$d^4k\,\theta(q_0-k_0)\,\delta((q-k)^2) = \frac{\pi}{4\nu}\,t\,dt\,\frac{d\beta}{\beta^2}\,\theta(-t)\,\theta(\beta-\omega) , \tag{5.11}$$

where $\nu = p\cdot q$ and the lower boundary of the t-integration region has been ignored in the scaling limit. The positivity of the mass of intermediate states in the quark-proton amplitudes also restricts the integration region to $\beta < 1$.

Now, the requirement that k^2 be small, along with the phase-space restriction $\beta > \omega$ from (5.11), causes the invariant $p\cdot k$ to be small also (in other words, when one parton is struck, the partons that remain behind form a state of limited mass). The only other invariant formed from k is $q\cdot k$, and it is determined by the δ function on the left-hand side of (5.11) to be $\frac{1}{2}q^2$. Thus, for the purposes of computing the traces in (5.7), it is adequate to approximate in the scaling limit

$$k_\mu \approx -\omega p_\mu . \tag{5.12}$$

The integrand in (5.7) is then dependent on k_μ only through the three scalar invariants (5.10a), (5.10b) along with $(q-k)^2$. This justifies the integration over the fourth variable in (5.11).

So, using (5.11) and (5.12), the amplitude (5.7) can be written as

$$W_{\mu\nu}^{ab} = \frac{1}{128\pi^2\nu}\int_{-\infty}^{0} t\,dt\int_{\omega}^{1}\frac{d\beta}{\beta^2}\left[\mathrm{tr}(M_1-\omega M_2)\,\lambda_a\lambda_b\,\mathrm{Tr}\not{p}\,\Gamma_\mu(\not{q}+\omega\not{p})\,\Gamma_\nu + \mathrm{tr}(\bar{M}_1-\omega\bar{M}_2)\,\lambda_b\lambda_a\,\mathrm{Tr}\not{p}\,\Gamma_\nu(\not{q}+\omega\not{p})\,\Gamma_\mu\right] . \tag{5.13}$$

Now, noting that

$$\lambda_a\lambda_b = (d_{abc}+if_{abc})\,\lambda_c , \tag{5.14}$$

the SU(3) traces in (5.13) can be written in terms of two nonets of quark-proton amplitudes M_a and $\bar{M}_a$ defined by the contraction

$$M_a(t,\beta,\omega) = \mathrm{tr}(M_1-\omega M_2)\,\lambda_a \tag{5.15}$$

and similarly for $\bar{M}_a$.

Finally, in order to make contact with the formalism of Sec. III we define the Laplace transforms

$$\mathfrak{M}_a(b,\beta,\omega) = \frac{1}{2\pi i}\int_{-i\infty}^{i\infty} t\,dt\,e^{-bt}M_a(t,\beta,\omega) . \tag{5.16}$$

With (5.14), (5.15), and (5.16), the expression (5.13) becomes

$$W_{\mu\nu}^{ab} = \frac{1}{128\pi^2\nu}\int_0^\infty\frac{db}{b}\int_\omega^1\frac{d\beta}{\beta^2}\left[(d_{abc}+if_{abc})\,\mathfrak{M}_c\,\mathrm{Tr}\not{p}\,\Gamma_\mu(\not{q}+\omega\not{p})\,\Gamma_\nu + (d_{abc}-if_{abc})\,\bar{\mathfrak{M}}_c\,\mathrm{Tr}\not{p}\,\Gamma_\nu(\not{q}+\omega p)\,\Gamma_\mu\right] . \tag{5.17}$$

The tensor $W_{\mu\nu}^{ab}$ is decomposed into invariant structure functions as follows:

$$\frac{1}{4\pi}W_{\mu\nu}^{ab} = \frac{1}{\nu}\left[p_\mu p_\nu - \frac{\nu}{q^2}(p_\mu q_\nu + q_\mu p_\nu) + \frac{\nu^2}{q^2}g_{\mu\nu}\right]F_2^{ab} - \frac{\nu}{q^2}\left(g_{\mu\nu}-\frac{q_\mu q_\nu}{q^2}\right)F_L^{ab} + \frac{i}{2\nu}\epsilon_{\mu\nu\alpha\beta}q^\alpha p^\beta F_3^{ab} + \cdots . \tag{5.18}$$

The remaining terms in (5.18) are not conserved in both indices and can be neglected in the scaling limit. Comparing (5.18) with (5.17), it is seen that the longitudinal scaling functions F_L^{ab} also vanish. The structure functions F_2^{ab} can be seen to arise from the product of two vector currents or of two axial-vector currents, whereas F_3^{ab} comes from one vector and one axial-vector current.

From (5.17) and (5.18) any electroproduction or neutrino-induced production structure function can be written as an integral over various combinations of the quark-proton amplitudes. Of particular interest in Sec. VI will be the neutrino and antineutrino functions

$$F_2^{\bar{\nu}p,\nu p}=\frac{\omega}{16\pi^3}\int_0^\infty\frac{db}{b}\int_\omega^1\frac{d\beta}{\beta^2}\left[\frac{\sqrt{2}}{\sqrt{3}}(\mathfrak{M}_0+\overline{\mathfrak{M}}_0)\pm(\mathfrak{M}_3-\overline{\mathfrak{M}}_3)+\frac{1}{\sqrt{3}}(\mathfrak{M}_8+\overline{\mathfrak{M}}_8)\right] \tag{5.19}$$

and

$$F_3^{\bar{\nu}p,\nu p}=\frac{-1}{16\pi^3}\int_0^\infty\frac{db}{b}\int_\omega^1\frac{d\beta}{\beta^2}\left[\frac{\sqrt{2}}{\sqrt{3}}(\mathfrak{M}_0-\overline{\mathfrak{M}}_0)\pm(\mathfrak{M}_3+\overline{\mathfrak{M}}_3)+\frac{1}{\sqrt{3}}(\mathfrak{M}_8-\overline{\mathfrak{M}}_8)\right]. \tag{5.20}$$

These four structure functions are seen to be determined by six quark-proton amplitudes. However, note that the two nonets M_a and $\overline{M}_a$ represent the coupling of bilocal currents to the proton. It is natural to suppose that this coupling is nonet-symmetric, specifically that

$$M_0=\sqrt{2}\,M_8 \tag{5.21}$$

and similarly for $\overline{M}$. As mentioned before, this corresponds to the physical assumption that the proton contains no strange quarks.

The integrals over each quark-proton amplitude are now determined in terms of the neutrino and antineutrino structure functions. Defining, for convenience,

$$I_a(\omega)=\frac{\omega}{2\pi^3}\int_0^\infty\frac{db}{b}\int_\omega^1\frac{d\beta}{\beta^2}\mathfrak{M}_a\,, \tag{5.22}$$

with a similar definition for $\overline{I}_a$, and also

$$F_\pm^{\bar{\nu}p,\nu p}=F_2^{\bar{\nu}p,\nu p}\pm\omega F_3^{\bar{\nu}p,\nu p}\,,$$

we can write

$$I_3=F_-^{\bar{\nu}p}-F_-^{\nu p}\,, \tag{5.23a}$$

$$\overline{I}_3=F_+^{\nu p}-F_+^{\bar{\nu}p}\,, \tag{5.23b}$$

$$I_8=\frac{1}{\sqrt{3}}(F_-^{\bar{\nu}p}+F_-^{\nu p}), \tag{5.23c}$$

$$\overline{I}_8=\frac{1}{\sqrt{3}}(F_+^{\bar{\nu}p}+F_+^{\nu p}). \tag{5.23d}$$

I_0 and $\overline{I}_0$ are $\sqrt{2}$ times I_8 and $\overline{I}_8$, respectively.

B. Lepton-pair production [13]

Now that we have obtained the relationship between the deep-inelastic scaling functions and the quark-proton amplitudes, it is a fairly simple matter to obtain an expression for the lepton-pair production cross section. The process is assumed to take place as shown in Fig. 7. Repeating the steps in Sec. IV leading up to (4.2) with the pion fields replaced by quark fields, the G function in this model is given in terms of the quark amplitudes defined in (5.5):

$$G(k,k',p_1,p_2)=[M_{\delta\alpha}^{ki}(p_1,k)\overline{M}_{\beta\gamma}^{jk}(p_2,k')+(p_1\rightarrow p_2)]\times(\gamma_\mu)_{\alpha\beta}(\gamma^\mu)_{\gamma\delta}\,Q^{ij}Q^{kl}\,, \tag{5.24}$$

where Q is the charge matrix

$$Q=\tfrac{1}{2}\left(\lambda_3+\frac{1}{\sqrt{3}}\lambda_8\right). \tag{5.25}$$

The Dirac indices can be sorted out by a Fierz rearrangement,

$$(\gamma_\mu)_{\alpha\beta}(\gamma^\mu)_{\gamma\delta}=(1)_{\alpha\delta}(1)_{\gamma\beta}-\tfrac{1}{2}(\gamma_\mu)_{\alpha\delta}(\gamma^\mu)_{\gamma\beta}-\tfrac{1}{2}(\gamma_5\gamma_\mu)_{\alpha\delta}(\gamma_5\gamma^\mu)_{\gamma\beta}-(\gamma_5)_{\alpha\delta}(\gamma_5)_{\gamma\beta}\,. \tag{5.26}$$

The last two terms in this expression vanish when contracted with the quark-proton amplitudes in (5.24) because of parity conservation. Also the contribution of the scalar term in (5.26) can easily be seen to give a contribution which is one order lower in s. Thus, the second term in (5.26) is the only one that survives.

The SU(3) indices in (5.24) can be sorted out in a similar way by writing

$$Q^{ij}Q^{kl}=\sum_{a,b}A_{ab}(\lambda_a)^{il}(\lambda_b)^{kj}\,, \tag{5.27}$$

where, by contracting both sides with appropriate λ's, we find

$$A_{00}=\tfrac{1}{9},\quad A_{33}=\tfrac{5}{36},$$
$$A_{03}=A_{30}=\tfrac{1}{36}\sqrt{6}\,,\quad A_{38}=A_{83}=\tfrac{1}{36}\sqrt{3}\,, \tag{5.28}$$
$$A_{08}=A_{80}=\tfrac{1}{36}\sqrt{2}\,,\quad A_{88}=\tfrac{1}{12}\,,$$

and all the rest are zero. The function G is then

$$G(t_1,t_2,\beta_1,\beta_2)=-4s\sum_{a,b}A_{ab}[M_a(t_1,\beta_1,\omega_1)\times\overline{M}_b(t_2,\beta_2,\omega_2)+(1\rightleftarrows2)]. \tag{5.29}$$

Now going back to Sec. III, expression (3.20), we can integrate over $q_\perp{}^2$ to get

$$\int_0^\infty dq^2\,W=\frac{1}{8(2\pi)^3s}\times\int_0^\infty\frac{db_1}{b_1}\frac{db_2}{b_2}\times\int_{\omega_1}^1\frac{d\beta_1}{\beta_1{}^2}\int_{\omega_2}^1\frac{d\beta_2}{\beta_2{}^2}\,\mathcal{G}(b_1,b_2,\beta_1,\beta_2)\,, \tag{5.30}$$

$\mathcal{G}$ being defined in terms of (5.29) via (3.14). The expression (5.30) is seen to involve the same integrals (5.22) over the Laplace-transformed quark-proton amplitudes as those which occur in the

deep-inelastic structure functions. This allows us to write the differential cross section as

$$\frac{d^2\sigma}{dq^2\,dy} = \frac{\pi\alpha^2}{24q^4}\sum_{a,b} A_{ab}[I_a(\omega_1)\,\bar{I}_b(\omega_2) + (1 \rightleftharpoons 2)]\,, \tag{5.31}$$

where the coefficients A_{ab} are given in (5.28), the quantities I_a and $\bar{I}_a$ are the combinations of neutrino structure functions shown in (5.23), and ω_1 and ω_2 are given in terms of $\omega = q^2/s$ and y by (4.17).

If (5.23) and (5.28) are inserted in (5.31), considerable simplification is obtained, giving

$$\frac{d^2\sigma}{dq^2\,dy} = \frac{\pi\alpha^2}{24q^4}\left[\tfrac{4}{9}F_-^{\bar{\nu}p}(\omega_1)\,F_+^{\nu p}(\omega_2) + \tfrac{1}{9}F_-^{\nu p}(\omega_1)\,F_+^{\bar{\nu}p}(\omega_2) + (1 \rightleftharpoons 2)\right]. \tag{5.32}$$

The individual terms in this expression can be interpreted as describing the annihilation of $\mathcal{P}$-type and $\mathfrak{N}$-type quarks with their corresponding antiquarks. Annihilation of λ quarks has been ignored by our nonet-symmetry assumption.

A detailed comparison of (5.32) with experiment must await more accurate data, both on neutrino scattering and on lepton-pair production. We can, however, make some rough estimates from presently available data. In particular, using the BNL data for lepton-pair production, we can estimate the important quantity B in neutrino scattering, defined as

$$B = -\int_0^1 \omega F_3^{\nu p}(\omega)\,d\omega \Big/ \int_0^1 F_2^{\nu p}(\omega)\,d\omega\,. \tag{5.33}$$

A similar quantity $\bar{B}$ is defined in terms of the $\bar{\nu}p$ structure functions.

Integrating (5.32) over rapidity, the mass distribution assumes the Drell-Yan scaling form

$$\frac{d\sigma}{dq^2} = \frac{1}{q^4}F(\omega)\,, \tag{5.34}$$

with

$$F(\omega) = \tfrac{1}{12}\pi\alpha^2\int_0^1 d\omega_1\,d\omega_2\,\delta(\omega_1\omega_2 - \omega) \times\left[\tfrac{4}{9}F_-^{\bar{\nu}p}(\omega_1)\,F_+^{\nu p}(\omega_2) + \tfrac{1}{9}F_-^{\nu p}(\omega_1)\,F_+^{\bar{\nu}p}(\omega_2)\right]. \tag{5.35}$$

To obtain an estimate of B, consider the zeroth moment of the Drell-Yan scaling function

$$\int_0^1 d\omega\,F(\omega)\,. \tag{5.36}$$

The calculation of (5.36) from the BNL data is fairly insensitive to the exact form of scaling function used to fit the data,

$$\int_0^1 d\omega\,F(\omega) = (5.0 \pm 0.5)\times 10^{-7} \tag{5.37}$$

[the error quoted is an estimate obtained by considering several different forms for $F(\omega)$ which give a reasonable fit to the data]. This is to be compared with the moment calculated from (5.35):

$$\int_0^1 F(\omega)\,d\omega = \tfrac{1}{12}\pi\alpha^2\left(\int_0^1 F_2^{\nu p}(\omega_1)\,d\omega_1\right) \times\left(\int_0^1 F_2^{\bar{\nu}p}(\omega_2)\,d\omega_2\right) \times\left[\tfrac{4}{9}(1+\bar{B})(1-B) + \tfrac{1}{9}(1+B)(1-\bar{B})\right]. \tag{5.38}$$

The experimental analysis of Perkins[14] gives the integrated F_2 for neutrino scattering averaged over neutron and proton. Using isospin symmetry to relate νn to $\bar{\nu}p$, Perkins's analysis gives

$$\int_0^1 (F_2^{\bar{\nu}p} + F_2^{\nu p})\,d\omega \approx 0.98 \pm 0.14. \tag{5.39}$$

Using quark-model arguments coupled with electroproduction data, another useful quantity is obtained[15]:

$$\int_0^1 \omega(F_3^{\nu p} - F_3^{\bar{\nu}p})d\omega = \bar{B}\int_0^1 F_2^{\bar{\nu}p}\,d\omega - B\int_0^1 F_2^{\nu p}\,d\omega \approx 0.24 \pm 0.12\,. \tag{5.40}$$

Finally, in order to obtain an estimate of B, let us suppose $\bar{B} \approx B$. Then using (5.39) and (5.40) to calculate the right-hand side of (5.38) in terms of B and comparing with the experimental value (5.37), we get

$$B \approx 0.84 \pm 0.06\,. \tag{5.41}$$

This is to be compared with the value obtained from Perkins's[14] analysis of neutrino data,

$$B = 0.86 \pm 0.04\,. \tag{5.42}$$

In spite of the inexact way in which the estimate (5.41) was extracted from the original formula (5.35), the agreement seems promising.[16] In particular, the fact that both estimates of B are fairly close to unity is significant. The value $B = \bar{B} = 1$ would indicate a complete absence of nonstrange antiquarks in the proton. Thus, from the point of view of the quark-parton model, the neutrino data and the lepton-pair production data seem to be in agreement in suggesting that the proton contains a rather meager portion of antipartons. Further verification of the relation (5.32), as well as of the scaling behavior (5.34) at different energies, will provide much more exacting tests of this model.

VI. BREMSSTRAHLUNG MODEL

Up to this point most of the dynamical considerations of this paper have been in the context of an-

nihilation models, in which a virtual particle from one proton annihilates a corresponding antiparticle from the other to produce the lepton pair. But, whether one thinks in terms of Feynman graphs or partons, another equally simple mechanism for producing lepton pairs suggests itself. This is a process in which the virtual photon is emitted from one of the protons, or from one of its partons, via a bremsstrahlung process. There are several features of such a model which make it an interesting object of study. Most importantly, it provides a mechanism for the production of lepton pairs with large transverse momentum. The cross section for the model studied here is nondecreasing, as $q_\perp^2$ becomes large. This behavior is of both theoretical and practical significance. As will be discussed in a future paper, the presence of a component of the cross section which does not fall off in $q_\perp^2$ [or which falls off slower than $(q_\perp^2)^{-1}$] reflects the existence of a light-cone singularity in the current product (2.3). From the practical side, such a transverse-momentum behavior may make it possible to study such processes even if they make up an insignificant part of the total cross section.

Another interesting feature of this model is that it satisfies current conservation in a nontrivial way. (This is in contrast to annihilation models, in which the only way to ensure gauge invariance is to impose a strong cutoff in the masses of the annihilating particles, keeping them close enough to their mass shells that current conservation is satisfied to leading order in s.) Its structure suggests that it would be an ideal laboratory for investigating the applicability of such ideas as current algebra and light-cone expansions to lepton-pair production. These subjects are currently under investigation and will not be discussed here. However, we venture one somewhat speculative comment about current conservation and the behavior of the total cross section for fixed q^2 in the limit $s \to \infty$. It was seen in Sec. IV [viz. (4.20) and (4.21)] that the cross section for an annihilation model grows in this limit like $\ln s$ (this is just the logarithmic multiplicity growth characteristic of multiperipheral models), provided only that the cutoff was strong enough, as defined by (4.19). But this was just the cutoff strength necessary to have the total cross section dominated by finite $q_\perp^2$. In view of the results of Sec. IV C, this also means that the masses t_1 and t_2 of the annihilating particles remain finite, and hence, that current is conserved to leading order in s. If, on the other hand, one allowed the cutoff to be less strong than (4.19) and ignored the fact that the model was no longer gauge-invariant, he would predict a cross section which grows like a power of s. There is an interesting parallel to this discussion in the bremsstrahlung model considered in this chapter, which consists of a gauge-invariant set of Feynman graphs. If one considers any of the graphs individually and calculates a cross section from it, the result will grow linearly in s for fixed q^2. But when the gauge-invariant set is added together, a cancellation occurs, and the cross section behaves like a constant in this limit. Thus, there is at least a *de facto* relationship in each of these models between the restrictions necessary to obtain gauge invariance and those necessary to avoid a power-law growth of the cross section in s at fixed q^2. This observation may be of relevance to the current-algebra considerations of Sanda and Suzuki[17] and the light-cone analysis of Brandt and Preparata.[18] Both of these authors predicted a linear growth of the cross section in s, but neither gave much consideration to the requirements of current conservation. Brandt and Preparata considered only scalar currents, and so any subtleties related to current conservation were ignored from the start. Sanda and Suzuki ignore current conservation in their use of the Low theorem to evaluate the two-particle matrix element of a single current. To do this, they must throw away pole terms, but these terms are not by themselves gauge-invariant (which is in fact the essential ingredient of the Low theorem).

It should be emphasized that the model considered in this section is not meant to be realistic, but rather is presented as the simplest alternative to annihilation models and as a possible starting point for investigations into the subjects mentioned in the previous paragraph. Thus, we eschew any comparison with experiment and are content to observe the qualitative features of the differential cross section. The model describes the scattering of two fermions with the emission of a massive virtual photon (lepton pair) from one of the fermion lines. The strong interactions are simulated by the exchange of a neutral vector gluon, with the gluon propagator being replaced by a pure exponential in order to give an elastic fermion-fermion cross section of the form

$$\frac{d\sigma_{el}}{dt} = \frac{g^4}{4\pi m^4} e^{\Omega t} . \tag{6.1}$$

In this expression, g is the fermion-gluon coupling, and m is a dimensional constant which will eventually be expressed in terms of the total elastic fermion-fermion cross section.

In this model there are all together the absorptive parts of 16 graphs. One is shown in Fig. 7 along with the momentum labels to be used. Then there are three more with both photons on the upper line, four similar ones with both photons on

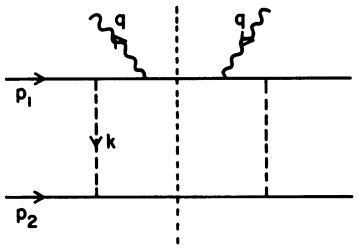

FIG. 7. A bremsstrahlung graph. Dotted line denotes absorptive part.

the lower line, and finally eight interference graphs where one photon is attached to the upper line and one to the lower line. Let us first dismiss the interference graphs by the following consideration: If this model is of physical interest, it will undoubtedly be in kinematical regions where $q_\perp^2$ is large. For this situation, it can be easily shown that it is impossible for both vector gluons to be near the mass shell. These graphs will therefore fall off in $q_\perp^2$, by virtue of the gluon-mass cutoff, and will be unimportant in the region of interest.

Now we need only consider the four graphs obtained by permutations of Fig. 7, the other four being available by substitution ($p_1 \rightarrow p_2$). These four graphs can be written by the standard rules as

$$W=\frac{g^4}{4\pi^2 m^4}\int d^4k\, D e^{\Omega k^2}\delta((p_1+k-q)^2)\,\delta((p_2-k)^2)\,. \tag{6.2}$$

Here the fermion mass has been ignored. The quantity D in (6.2) includes Dirac matrix traces as well as fermion propagators. One of the more impeachable assumptions of this model will be that the amplitude is not cut off in the mass of the off-shell fermion. A rationale, if not a justification, for this assumption is that, in order to emit a massive virtual photon, the fermion must be far off shell between the photon and gluon vertex. A model which was cut off in the fermion mass would therefore be of little interest.

In order to evaluate the phase-space integral (6.2) by the method of Sec. III, we define the invariant integration variables

$$t_1=(k+q)^2, \tag{6.3a}$$

$$t_2=k^2, \tag{6.3b}$$

$$\beta_1=\frac{t_1}{2p_1\cdot(k+q)}\,, \tag{6.3c}$$

$$\beta_2=\frac{-t_2}{2p_2\cdot k}\,. \tag{6.3d}$$

To find the function G which appeared in Sec. III, simply compare (6.2) with (3.4). This function must then be Laplace-transformed to find $\mathcal{G}$ as in (3.14). But first the Dirac traces must be expanded and the various pieces of D added together. This is rather tedious, and the details are not of sufficient interest to include here. Since a cutoff in the gluon mass t_2 has been assumed, it suffices to write the combined D of the four graphs as an expansion in t_2:

$$D=D_0+D_1t_2+\cdots\,. \tag{6.4}$$

At first it would seem that only the first term in (6.4) need be kept. But actually there is a certain cancellation, which will be detailed shortly, that causes the term of leading order in s from each graph to cancel when they are added together. Thus, only the second leading term from D_0 survives, and in order to obtain the whole cross section one must include the leading term coming from D_1.

Let us now focus on the first term in (6.4), which is, after some algebra,

$$D_0=\frac{8s\omega}{(\omega_2-\omega)^2(s\omega_2-t_1)^2}\,[s\omega_\perp+(1-\omega_1)t_1]^2. \tag{6.5}$$

An important feature of this expression is that it vanishes at

$$t_1=\frac{-\omega_\perp}{1-\omega_1}\,s. \tag{6.6}$$

The importance of this fact arises from the restrictions of phase space. Recall that the determinant H introduced in Sec. III and the Appendix has the property that $H<0$ defines the physical region. Taking the expression (A5) for H and setting $\beta_1=\beta_2=1$, which arises from the δ functions in (6.2), gives

$$\frac{1}{16s^2}H=[(1-\omega_1)t_1+(1-\omega_2)t_2+q_\perp^2]^2 - 4[(1-\omega_1)(1-\omega_2)-\omega_\perp]\,t_1t_2\,. \tag{6.7}$$

It is clear that as $t_2\rightarrow 0$, t_1 is restricted to be at precisely the value (6.5) which causes D_0 to vanish. This results in a cross section which is constant in s instead of linearly growing. The calculation of this piece of W is now a fairly straightforward application of the formalism of Sec. III. The exact formula (3.18) must be used since we are interested in finite $\omega_\perp$. The Laplace-transformed function is

$$\mathcal{G}_0=\frac{32\pi^2g^4s\omega(1-\omega_1)^2}{(\omega_2-\omega)^2m^4} \times\delta(1-\beta_1)\delta(1-\beta_2)\delta(b_2-\Omega)I\,, \tag{6.8}$$

where

$$I=\delta(b_1)-\frac{2s(\omega_2-\omega)}{(1-\omega_1)}\theta(b_1)e^{-b_1 s\omega_2}+\frac{s^2(\omega_2-\omega)^2}{(1-\omega_1)^2}b_1\theta(b_1)e^{-b_1 s\omega_2}\,. \tag{6.9}$$

The integration over b_1 in (3.18) is easily carried out by noting that, whereas $b_2=\Omega$, the value of b_1 is effectively restricted to be of order $1/s$, allowing an expansion of the integrand in powers of b_1/b_2. This is valid so long as we stay away from the extreme corner of phase space where $\omega_2\approx\omega$, $\omega_1\approx 1$, and $\omega_\perp\approx 0$, where $\approx$ means that the difference between the two quantities is of order $(\Omega s)^{-1}$. Thus the contribution to W of the first term in (6.4) is

$$W_0=\frac{4\sigma_{el}\omega}{s\Omega(\omega_2-\omega)^4}\omega_\perp[(1-\omega_1)(1-\omega_2)-\omega_\perp]\,. \tag{6.10}$$

The fact that this piece of W gives a negative contribution to the cross section [note the minus sign in (2.5)] underscores the necessity of including the second term in (6.4). Calculation of D_1 is tedious but straightforward [it is only necessary to evaluate D_1 for the particular value of t_1 given by (6.6)], and the resulting contribution to W is easily evaluated with the formalism of Sec. III. It is

$$W_1=\frac{-\sigma_{el}}{\Omega s(1-\omega_1)^2(\omega_2-\omega)^2}\times\{[1+(1-\omega_1)^2][(1-\omega_1-\omega_2+\omega)^2+(1-\omega_1)^2]-2\omega\omega_\perp(1-\omega_1)\}\,. \tag{6.11}$$

Combining (6.10) and (6.11) gives a negative-definite result for W,[19]

$$W=\frac{-\sigma_{el}}{\Omega s(1-\omega_1)^2(\omega_2-\omega)^4}\times[(1-\omega_1)^2+(1-\omega_1-\omega_2+\omega)^2]\times[(1-\omega_1)^2\omega_2{}^2+(\omega_2+\omega\omega_1-2\omega)^2]\,. \tag{6.12}$$

Integrating this expression over the photon three-momentum with fixed q^2 [cutting off the integration for $\omega_2-\omega\lesssim O(1/\Omega s)$], one finds that the cross section $d\sigma/dq^2$ behaves as a constant in the limit $s\to\infty$, q^2 fixed, in accord with our previous discussion.

VII. CONCLUSION

The study of lepton-pair production in hadron-hadron collisions may provide some important clues about the structure of hadrons and about the range of applicability of several popular theoretical constructs, e.g., partons, multiperipheralism, current algebra, and light-cone dominance. In this paper, the consequences of some representative models were explored in an attempt to determine what physics might be indicated by present and future experimental data. It was found that the assumptions contained in each of these models could be most easily expressed in terms of a function G defined by (3.5), (3.3), and (3.2). The phase-space considerations of Sec. III were carried out in a model-independent way in the hope that they will be of some practical utility even if the models studied here prove inadequate.

Each of the models gives detailed predictions at all large values of s and is thus highly vulnerable to experiment. The pion-annihilation model gives an acceptable one-parameter description of the Brookhaven data[1] for values of q^2 below 6 GeV^2, but appears to be in trouble at higher values of q^2 if the pion electromagnetic form factor continues to fall as fast as (4.22). The quark-annihilation model, combined with the assumption that there are few strange quarks in the proton, gives a relationship between lepton-pair production and neutrino structure functions, the first moment of which is in excellent agreement if the quarks are assumed to have no color. The colored-quark model gives much poorer agreement.

Regarding annihilation models, it is interesting to note that should some such model prove worthy of being taken seriously, there is a simple way to determine the spin of the annihilating particles. Thinking in parton-model terms, we can assume that the annihilating partons have limited transverse momentum, and thus at large q^2 they are, to a good approximation, moving longitudinally in their center-of-mass system. Denoting by θ the angle between the beam axis and one of the leptons in the center-of-mass system of the lepton pair, the distribution in θ will be determined by the spin of the partons. Spin-0 partons would give a $\sin^2\theta$ distribution, whereas spin-$\frac{1}{2}$ partons (assumed bare) would give $1+\cos^2\theta$.

The bremsstrahlung model was studied more as a prototype than as a realistic model. The qualitative features of the cross section obtained may be of some experimental relevance, particularly if it is found that a component of the cross section persists out to finite values of $q_\perp{}^2/s$. Perhaps of more importance than the result was the cancellation which occurred among a certain gauge-invariant set of graphs, reducing the high-energy behavior by one power of s. The nature of the cancellation emphasizes the importance of taking proper account of the restrictions of phase space and gauge invariance. This model suggests itself as a natural laboratory for testing various arguments about light-cone behavior[14] and current algebra.[13]

ACKNOWLEDGMENTS

I would like to thank my colleagues at UCLA, where most of this work was completed, and in particular, Professor J. J. Sakurai and Professor J. M. Cornwall for numerous fruitful discussions and many invaluable suggestions.

APPENDIX

The determinant H which appears in (3.9) can be expressed in terms of invariants by multiplying the Jacobian (3.8) by its transpose. For convenience, we introduce the following auxiliary notation:

$$\alpha_1 = 1 - \frac{\omega_1}{\beta_1}, \tag{A1}$$

$$\alpha_2 = 1 - \frac{\omega_2}{\beta_2}, \tag{A2}$$

$$\lambda = (\beta_1 - \omega_1)(\beta_2 - \omega_2), \tag{A3}$$

$$R = [\omega_\perp(\lambda - \omega_\perp)]^{1/2}. \tag{A4}$$

After considerable algebra, H can be written as

$$H = 16s^2\left[(\alpha_1 t_1 + \alpha_2 t_2 + q_\perp^2)^2 + 4\left(\frac{\omega_\perp}{\beta_1\beta_2} - \alpha_1\alpha_2\right) t_1 t_2\right]. \tag{A5}$$

Now make the change of variables $(t_1, t_2) \to (r, \theta)$, where

$$t_1 = \frac{s}{2\alpha_1}\left[\left(\frac{\lambda}{\omega_\perp}\right)^{1/2} r\cos\theta + \left(\frac{\lambda}{\lambda - \omega_\perp}\right)^{1/2} r\sin\theta - \lambda\right], \tag{A6}$$

$$t_2 = \frac{s}{2\alpha_2}\left[\left(\frac{\lambda}{\omega_\perp}\right)^{1/2} r\cos\theta - \left(\frac{\lambda}{\lambda - \omega_\perp}\right)^{1/2} r\sin\theta - \lambda\right]. \tag{A7}$$

The determinant H now takes the simple form

$$H = 16s^4(r^2 - R^2). \tag{A8}$$

The integral (3.16) is now over a circle,

$$I = \frac{\beta_1\beta_2}{8R}\int_0^R \frac{r\,dr}{(R^2 - r^2)^{1/2}}\int_{-\pi}^{\pi} d\theta\, e^{b_1 t_1 + b_2 t_2}, \tag{A9}$$

where t_1 and t_2 are given by (A6) and (A7). The integral (A9) is now carried out using the identities

$$\int_{-\pi}^{\pi} d\theta\, e^{\lambda_1\cos\theta - \lambda_2\sin\theta} = 2\pi I_0((\lambda_1^2 + \lambda_2^2)^{1/2}) \tag{A10}$$

and

$$\int_0^R \frac{r\,dr}{(R^2 - r^2)^{1/2}} I_0(ar) = \frac{1}{a}\sinh(aR). \tag{A11}$$

From (A10) and (A11), the expression (A9) can be evaluated, giving (3.17).

---

*Work supported in part by the U. S. National Science Foundation Grant No. GP 32998X.

[1]J. H. Christenson, G. S. Hicks, L. M. Lederman, P. J. Limon, and B. G. Pope, Phys. Rev. Lett. 25, 1923 (1970); Phys. Rev. D 8, 2016 (1973).

[2]R. L. Jaffe, Phys. Rev. D 5, 2622 (1972).

[3]S. D. Drell and T.-M. Yan, Phys. Rev. Lett. 25, 316 (1970); Ann. Phys. (N.Y.) 66, 578 (1971).

[4]S. M. Berman, D. J. Levy, and T. L. Neff, Phys. Rev. Lett. 23, 1363 (1969).

[5]This model was suggested to me as an object of study by J. J. Sakurai.

[6]After completion of this work, it was brought to my attention that a very similar model has been studied by K. Subbarao [Phys. Rev. D 8, 1498 (1973)]. This author has also considered nucleon-pole terms in which the photon is at the end of the multiperipheral chain. Such terms may be of importance in the kinematic extremities ω_1 or $\omega_2 \approx 1$, but any quantitative estimate of their relative importance would require a model for the off-shell nucleon-nucleon forward amplitude. One possibility is to assume a cutoff in the nucleon mass, similar to (4.6) for the π-p amplitude. The contribution of the nucleon-pole terms to $d\sigma/dq^2$ would then vanish relative to the pion-annihilation component in the limit $s, q^2 \to \infty$, fixed ω (though they may still contribute to $d\sigma/d^4q$ near the kinematic limits). The other possibility is that such a process is not cut off in nucleon mass. The bremsstrahlung model discussed in Sec. VI can be viewed as the simplest gauge-invariant model for such a possibility.

[7]V. Silvestrini, in *Proceedings of the XVI International Conference on High Energy Physics, Chicago-Batavia, Ill., 1972*, edited by J. D. Jackson and A. Roberts (NAL, Batavia, Ill., 1973), Vol. 4, p. 1.

[8]The experimental longitudinal momentum cut at 12 GeV/c has also been taken into account in Fig. 4.

[9]Our presumptuous assumption here is that the use of the modified scaling variable (4.24) will legitimatize a comparison of our essentially asymptotic considerations with the decidedly nonasymptotic Brookhaven data. For a more detailed discussion and application of this "duality" principle, see J. J. Sakurai and H. B. Thacker, Nucl. Phys. B (to be published).

[10]This relates to the rather peculiar final-state hadron distribution predicted by this model. For large q^2 and s, the two subsets of hadrons will be separated by a gap in that part of longitudinal phase space occupied by the virtual photon. As q^2 increases, the gap widens and the two hadronic subsets are forced to opposite ends of the rapidity plot. The same conclusion does not apply to the quark-annihilation model studied in Sec. V since, in order to avoid fractionally charged subsets, one must invoke some mechanism by which the outgoing quarks "grow tails" back to the central region, thus permitting communication between the subsets. See Min-Shih Chen, Phys. Rev. D 9, 1453 (1974).

[11]E. Etim, M. Greco, and Y. N. Srivastava, Phys. Lett.

41B, 507 (1972).
[12]P. V. Landshoff and J. C. Polkinghorne, Nucl. Phys. B33, 221 (1971); J. Kuti and V. F. Weisskopf, Phys. Rev. D 4, 3418 (1971).
[13]The analysis in this section was carried out in collaboration with J. M. Cornwall.
[14]D. H. Perkins, in *Proceedings of the XVI International Conference on High Energy Physics, Chicago-Batavia, Ill., 1972,* edited by J. D. Jackson and A. Roberts (NAL, Batavia, Ill., 1973), Vol. 4, p. 189.
[15]C. H. Llewellyn Smith, Phys. Rep. 3C, 261 (1972).
[16]It is interesting to note that, had we assumed that quarks came in three different colors, the expressions (5.32), (5.35), and (5.37) would have an extra factor of $\frac{1}{3}$ on the right-hand side. In that case, assuming (5.37), (5.39), (5.40), and $B=\bar{B}$, it is not possible to satisfy (5.38) with any real value of B. The agreement between (5.41) and (5.42) could therefore be interpreted as evidence against colored quarks and in favor of the old-fashioned gray variety.
[17]A. I. Sanda and M. Suzuki, Phys. Rev. D 4, 141 (1971).
[18]R. A. Brandt and G. Preparata, Phys. Rev. D 6, 619 (1972).
[19]This result differs from that given in Ref. 4, though the latter calculation was not given in sufficient detail to pinpoint the discrepancy.

PHYSICAL REVIEW D VOLUME 9, NUMBER 9 1 MAY 1974

Diffractive behavior of deep-inelastic electroproduction in a resonance model

C. A. Dominguez and H. Moreno
Departamento de Física, Centro de Investigación y de Estudios Avanzados del Instituto Politécnico Nacional, Apartado Postal 14-740 Mexico 14, D. F.
(Received 28 November 1973)

The diffractivelike as well as the nondiffractive behavior of the structure functions of the nucleons is explained in terms of a resonance model in which not all the form factors have the same Q^2 dependence. The most important results of such a model are the following: (i) νW_2 tends to a constant in the Bjorken limit as $\omega' \to \omega \to \infty$. (ii) For $\omega' \to 1$ the Drell-Yan-West relation is obtained. (iii) The difference between proton and neutron structure functions, as well as their ratio, can be properly explained. (iv) For ν and Q^2 large but finite νW_2 falls like $1/\omega'$ for large ω'. (v) The model has only two parameters to account for F_{2p}, $F_{2p}-F_{2n}$, and F_{2n}/F_{2p}. A very good agreement with present experimental data is obtained in all three cases. (vi) A breakdown of scaling is predicted for any finite energy, though in the Bjorken limit the structure functions do scale.

INTRODUCTION

Deep-inelastic electroproduction experiments have provided important insight into the structure of the nucleons.[1] Among the prominent features of the data[2] one notes (i) a very large cross section, (ii) consistency with scaling behavior,[3] (iii) a correlation between electroproduction of resonances and the deep-inelastic regime,[4] and (iv) a significant nondiffractive behavior as evidenced by experiments measuring the difference between proton and neutron structure functions.[5] The first three features have been related previously[6,7] in the context of a model where the nucleon structure functions were expressed, in the deep-inelastic limit, as a sum of resonant contributions only. We shall briefly review the prominent steps of Ref. 6 since they constitute the basis of the model to be discussed in this paper.

On the assumption that in the deep-inelastic limit νW_2 can be expressed purely as a sum of resonant contributions, one has in the zero-width approximation

$$\nu W_2(q^2,\nu) = Q^2 \sum_f g^2(Q^2, m_f^2)\delta(m^2-m_f^2), \tag{1}$$

where q^2 = (mass)^2 of the exchanged photon, $Q^2=-q^2$, ν = energy transfer in the lab system, $m^2=(p+q)^2$ where p is the four-momentum of the nucleon, and f stands for the observed final states in electroproduction. The function $g(Q^2, m_f^2)$ is the effective form factor of the photon–nucleon–final-state vertex.

In the case of elastic scattering one has $m_f^2=M^2$ = (mass)^2 of the nucleon, and

$$\nu W_2(q^2,\nu) = Q^2 g^2(Q^2,M^2)\delta(2M\nu-Q^2), \tag{2}$$

with

$$g^2(Q^2,M^2) = \frac{G_E^2(Q^2)+(Q^2/4M^2)G_M^2(Q^2)}{1+Q^2/4M^2} \underset{Q^2\ \text{large}}{\sim} G_M^2(Q^2). \tag{3}$$

It is important to note that for a missing mass $W>2$ GeV one does not see distinct contributions coming from individual resonant states, while for